Properties and Calibration of MEMS and Piezoactuated Fabry-Perot Spectral Imagers

EUFAR Joint Expert Working Group Meeting: Imaging Spectroscopy Sensors, Calibration/ Validation, and Data Processing, Edinburgh, UK, 14th April 2011.

Heikki Saari

VTT Technical Research Centre of Finland

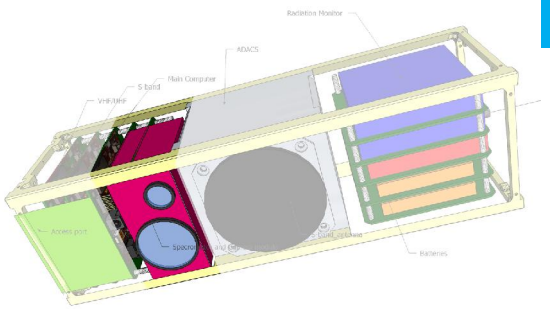

Outline

- Introduction and classification of imaging spectrometers
- Overview of the VTT Fabry-Perot Interferometer (FPI) – technologies
- Fabry-Perot Interferometer principle and spectroscopy applications
- FPI hyperspectral imager major characteristics and operation modes
- The Piezo-actuated FPI component and its controlling
- VTT's Surface Micro-Machined MEMS FPI Structure
- World's first MEMS FPI Spectral Imager
- VTT UAS FPI VIS-VNIR Spectral Camera for forest and agriculture applications
- FPI based spectral camera F-number and throughput
- Mathematical description of the FPI Spectral Imager concept
- Calibration of the FPI Hyperspectral Imager
- Conclusions and future plans
- Additional slides on the-state-of-the-art of the hyper and multispectral imaging technology and on planned UAV applications of FPI spectral imager

Classification of imaging spectrometers for remote sensing applications

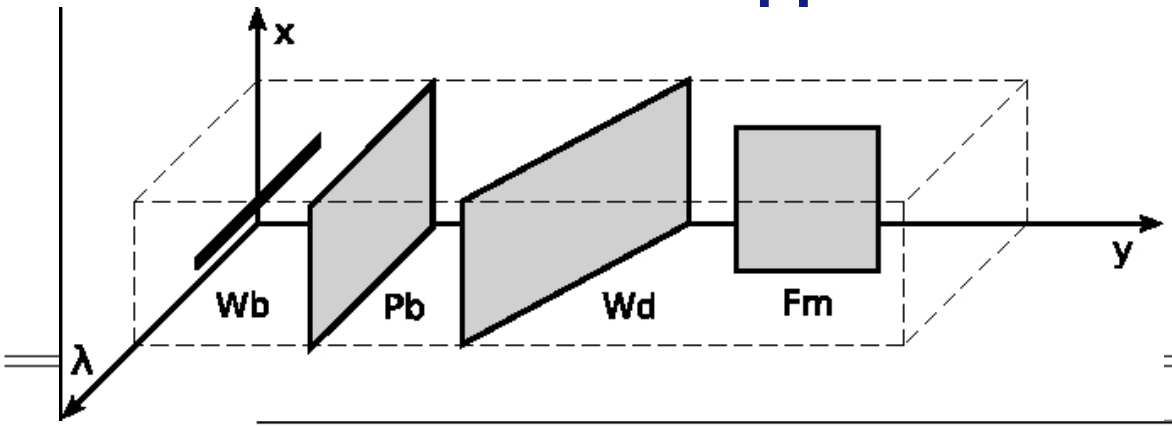

	Whiskbroom	Pushbroom	Windowing	Framing
Spectral	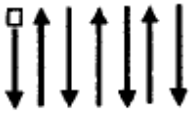	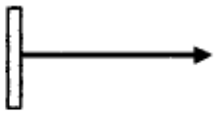	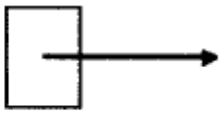	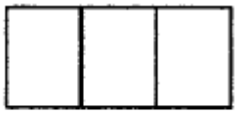
Filtering	• Multiband radiometer	• (No known examples)	• Filter array • Wedge filter • Linear variable filter	• Band-sequential • Filter wheel • Tunable filter (AOTF or LCTF)
Dispersive	• Grating or prism	• Grating or prism	• (No known examples)	• Image slicer • Tomographic
Interferometric	• Traditional FTS • Point FTS (Michelson)	• Static FTS (Sagnac)	• Static FTS (Mach-Zender, Sagnac)	• Traditional FTS (Michelson)

Ref. X. Prieto-Blanco, C. Montero-Orille, B. Couce, R. de la Fuente, "Optical configurations for Imaging Spectrometers, Comput. Intel. For Remote Sensing, SCI 133, pp. 1-25, 2008 Springer-Verlag, Heidelberg 2008.

Ref. R. Sellar&G. Boreman, "Classification of imaging spectrometers for remote sensing applications", Opt.Eng. 44(1), Jan 2005.

Overview of the VTT Fabry-Perot Interferometer – technologies

- **Microelectromechanical components (MEMS)**
  - Development started 1990 / 1991, CARBOCAP® -production at Vaisala / VTT 1997
  - Novel technologies: ALD, Si_3N_4, etc.
  - Small, robust, cheap, high volumes
  - Wavelength ranges 350 nm – 14000 nm
- **Piezo-components**
  - More transmitted light, large range of wavelengths
  - Small and medium series with apertures from 3 mm to 50 mm.
  - Fits well to imaging systems

- VTT owns IPR of several Fabry-Perot inventions

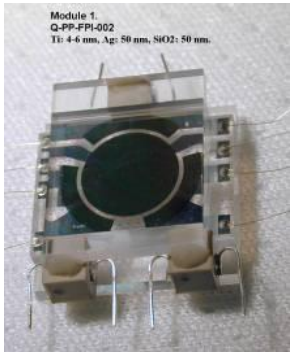

Piezo-actuated Fabry-Perot interferometer modules

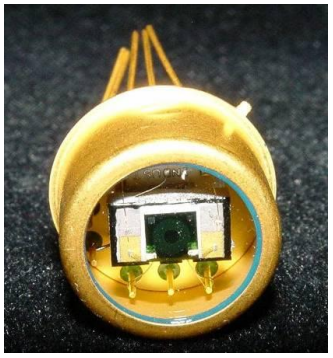

Detector modules including a Fabry-Perot interferometer detector and optionally cooling.

Filter chips, 3x3 mm^2

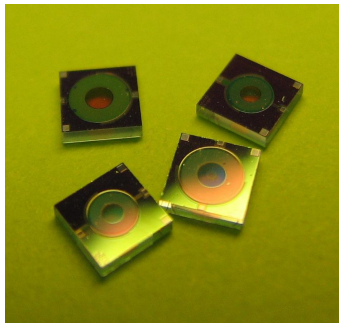

Tunable band-pass filters (350 – 14000 nm)

Fabry-Perot Interferometer and Spectroscopy

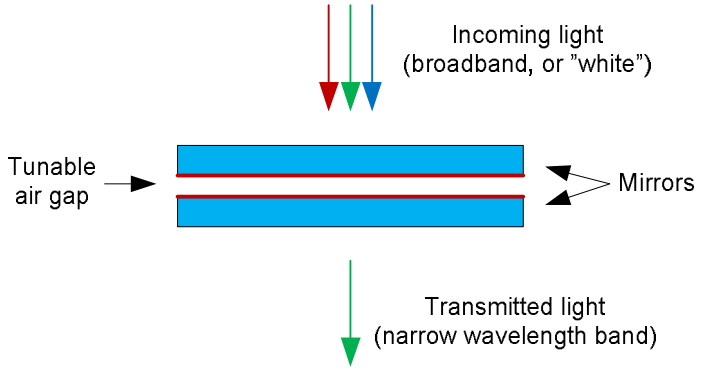

- Interference created by two reflective surfaces
- Usage: Tunable band-pass filter

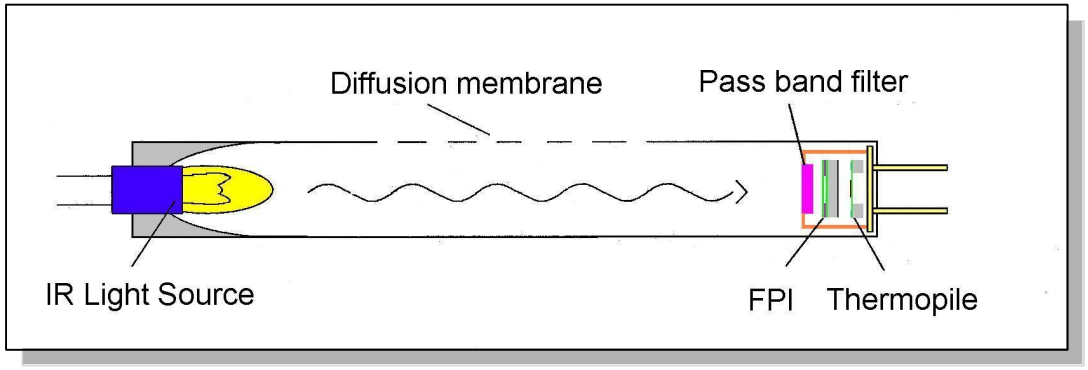

'Fingerprint' of Ethanol

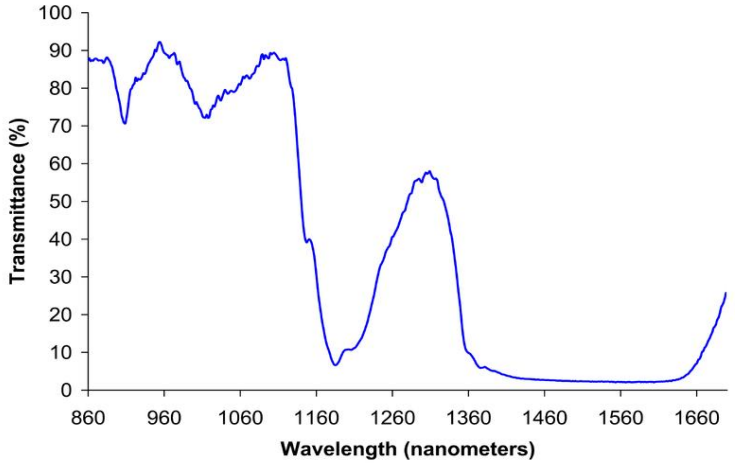

Fabry-Perot Interferometer (FPI) and principle of hyperspectral imaging based on it

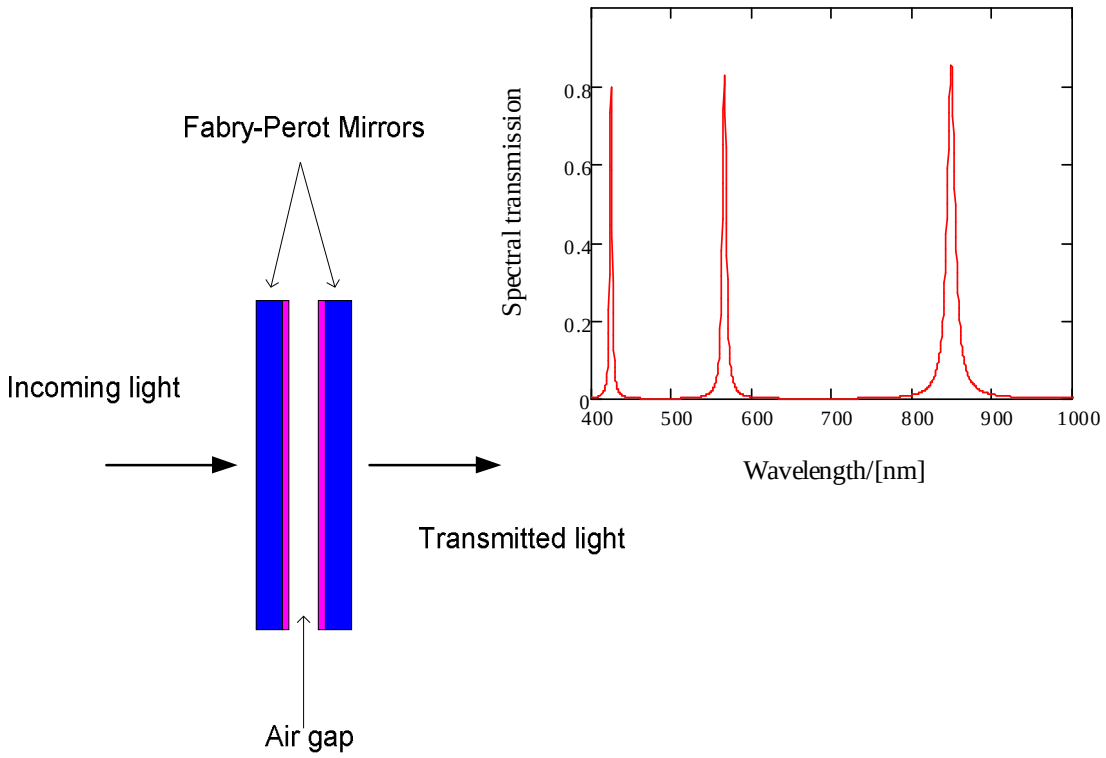

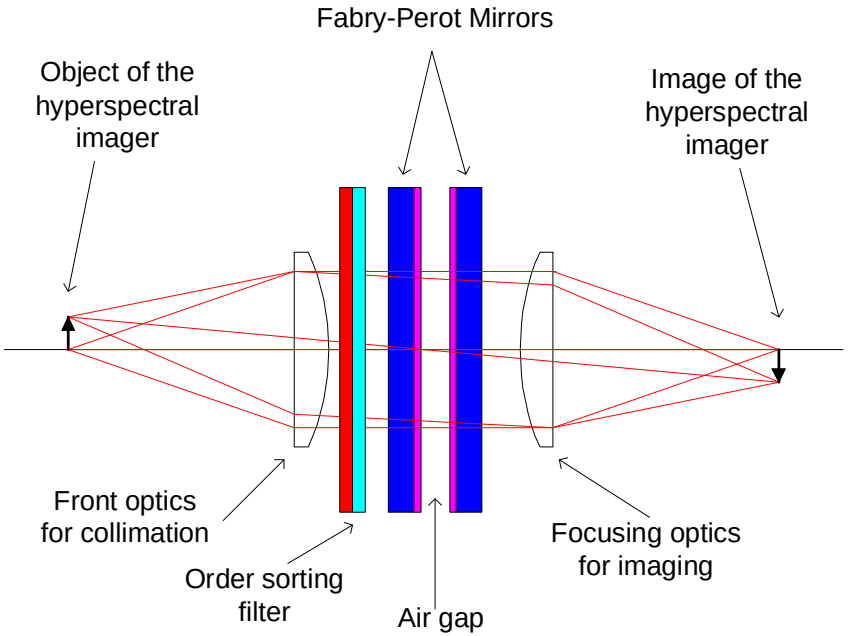

The Fabry-Perot Interferometer based hyperspectral imager concept.

FPI multispectral image sensor hyperspectral imager principle - Matching three Fabry-Perot Interferometer orders to a R-, G-, and B-pixels

Transmission of the Fabry-Perot Interferometer at air gap value of 1100 nm

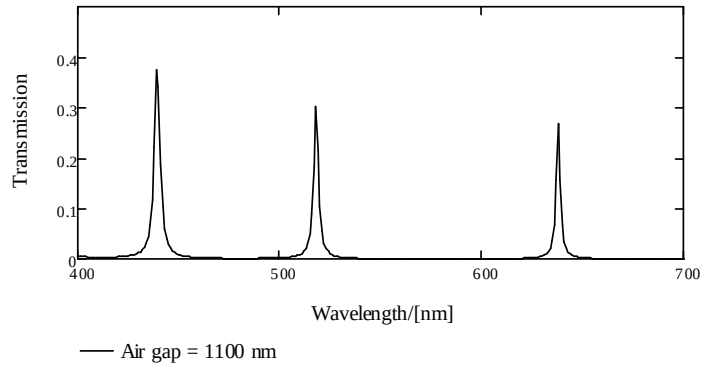

Quantum efficiency of CMOS RGB image sensor MT009V022

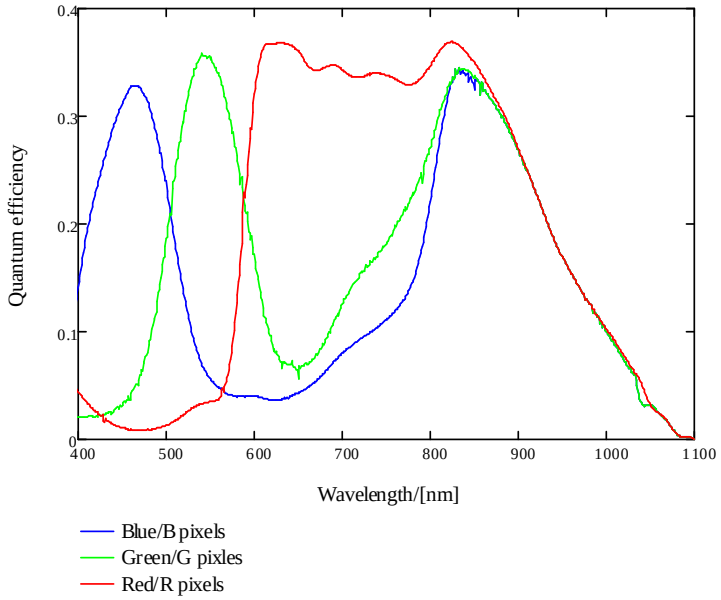

Combined Quantum efficiency of the Fabry-Perot Interferometer at air gap 1100 nm and the CMOS RGB image sensor MT009V022

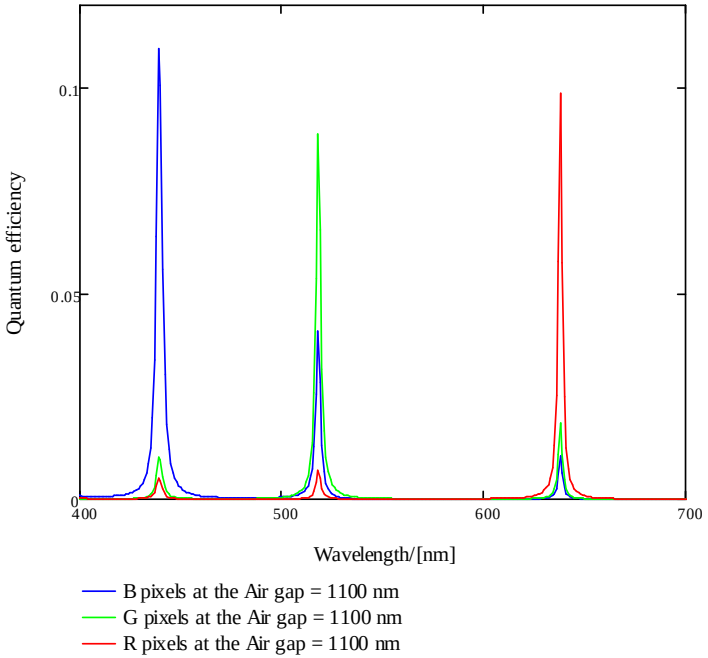

FPI hyperspectral imager major characteristics

Parameter	Typical value for Vis-VNIR	Typical value for SWIR
Visible-VNIR	400 – 1000 nm	900 – 2500 nm
Spectral resolution	3 - 11 nm @ FWHM	8 - 30 nm @ FWHM
Spectral step	< 1 nm	< 1 nm
Spectral instability	< 1 nm	< 1 nm
F-number @ 5 max FPI ray angle	< 2.8	< 2.8
F-number @ 10 max FPI ray angle	< 1.0	< 1.0
Average FPI transmission with metallic mirrors	25 %	25 %
Average FPI transmission with dielectric mirrors	80 %	80 %
Default spectral image dimensions	640 x 480 pixels	384 x 288 pixels
Maximum spectral image size	2592 x 1944 pixels	512 x 512 pixels
Recording time for 100 layer data cube	< 1.0 s	< 1.0 s
Dimensions	< 65 x 65 x 130 mm	< 150 x 100 x 200 mm
Weight	< 400 g	< 2.0 kg
Power consumption	< 3 W	< 25 W

FPI hyperspectral imager operation modes

- Tunable FPI filter camera utilizing only one FPI order at a time for example VNIR camera for 700 – 1000 nm with air gap range 520 – 880 nm, res. 9..11 @ FWHM or Vis-VNIR camera for 550 – 770 nm air gap range 360 – 560 nm, res. 12..15 @ FWHM
- False color imager with relatively narrow Green, Red and VNIR pass bands with +5 Mpix resolution (see next slide)
- The FPI camera can be used as a tunable multispectral imager with +5 Mpix resolution by taking images in sequence at the selected spectral bands. Three 5 Mpix images can be recorded in typically in less than 0.3 s.

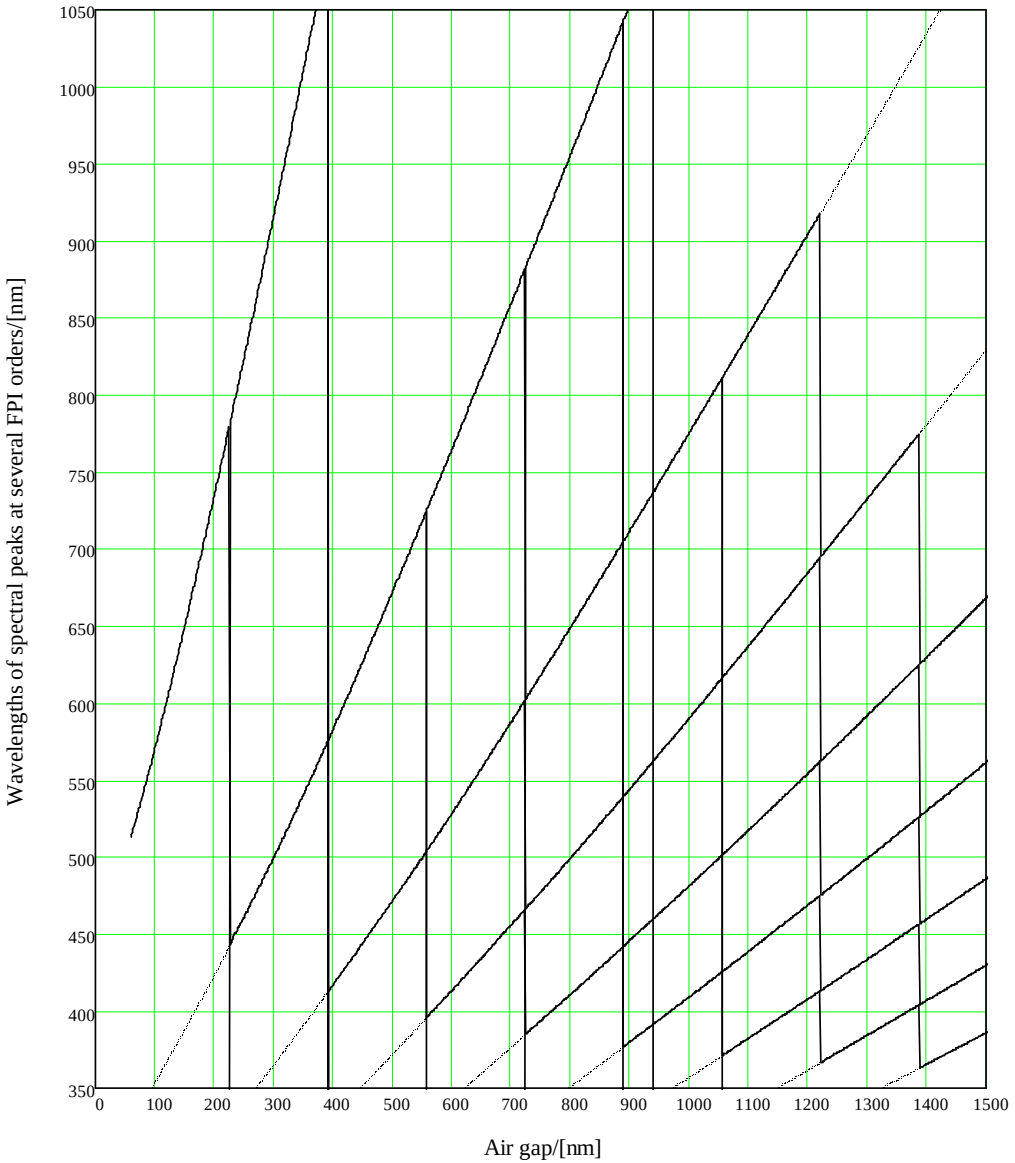

False color imager with relatively narrow Green, Red and VNIR pass bands

- The FPI spectral camera operates like a normal false color camera except the green (G), red (R) and VNIR spectral bands are narrower.
- An example of the measured spectral transmissions of the FPI module at air gap values of 1000 nm and 1500 nm are shown on the right.
- The spectral bands used in the false color imaging at the air gap value 1500 nm are:
  - G: 560 nm @ 10 nm FWHM
  - R: 670 nm @ 10 nm FWHM
  - VNIR: 845 nm @ 10 nm FWHM

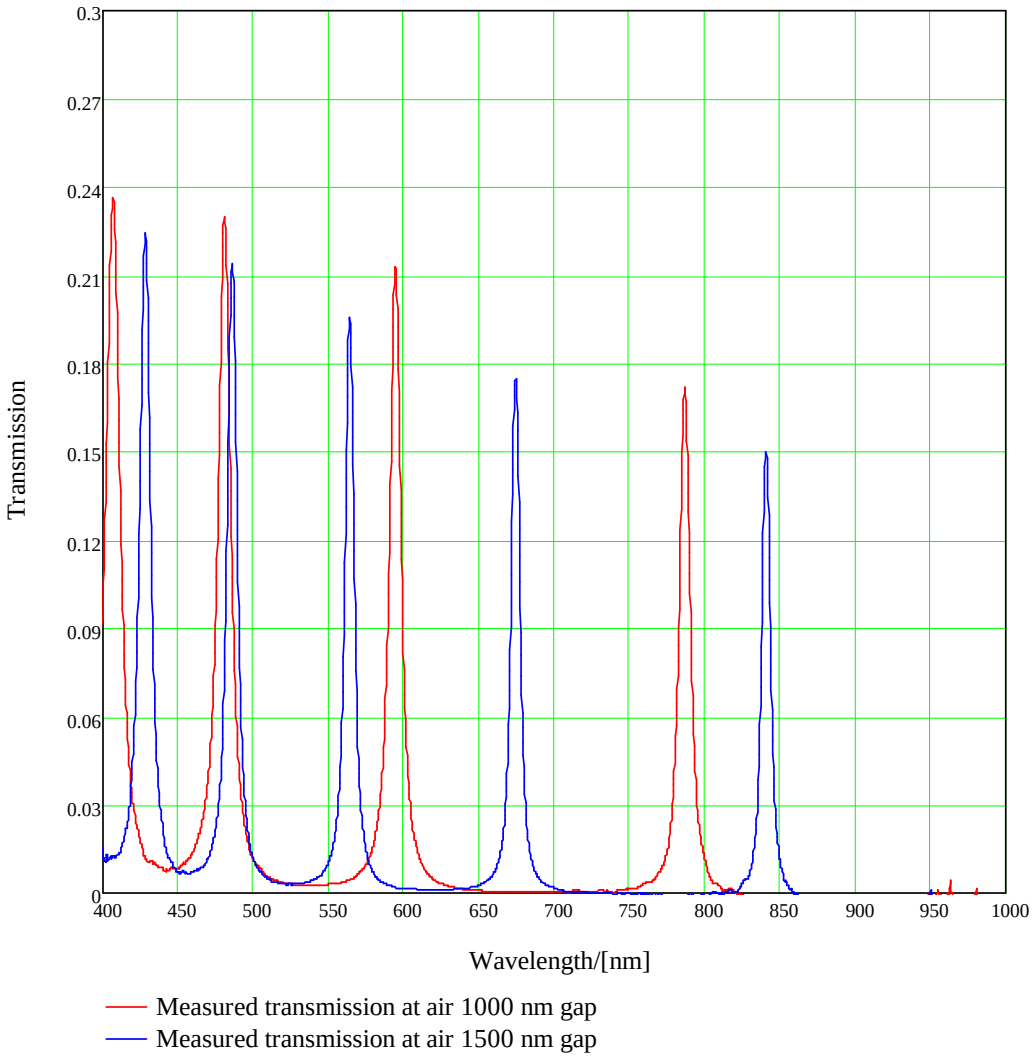

The Piezo-actuated Fabry-Perot Interferometer component and its controlling

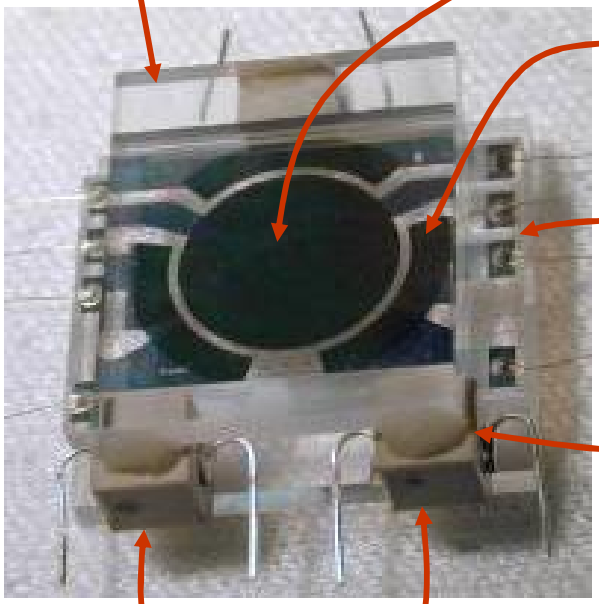

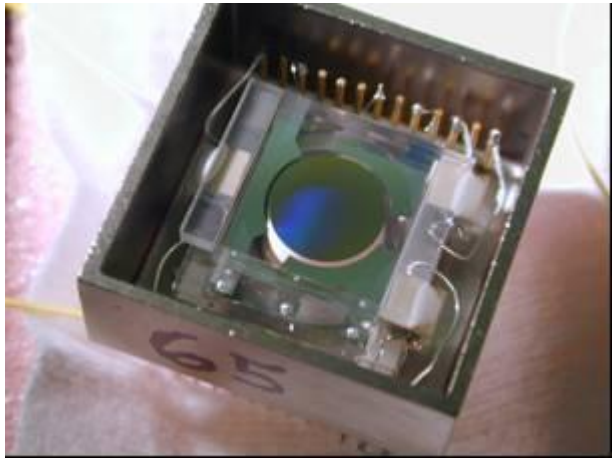

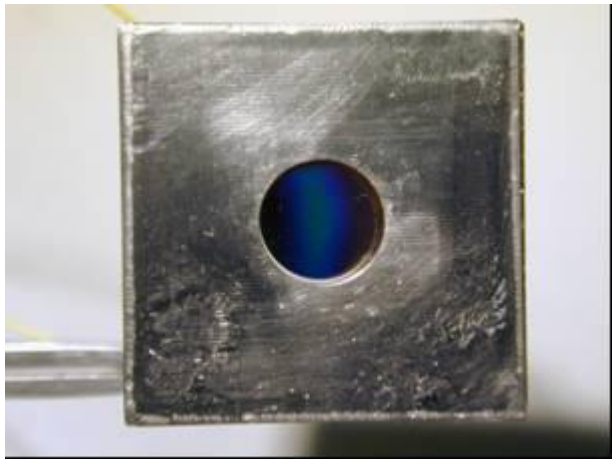

Hermetically packaged Piezo actuated FPI

=> FPI cavity stays parallel

Piezo Actuated Fabry-Perot Interferometer control electronics

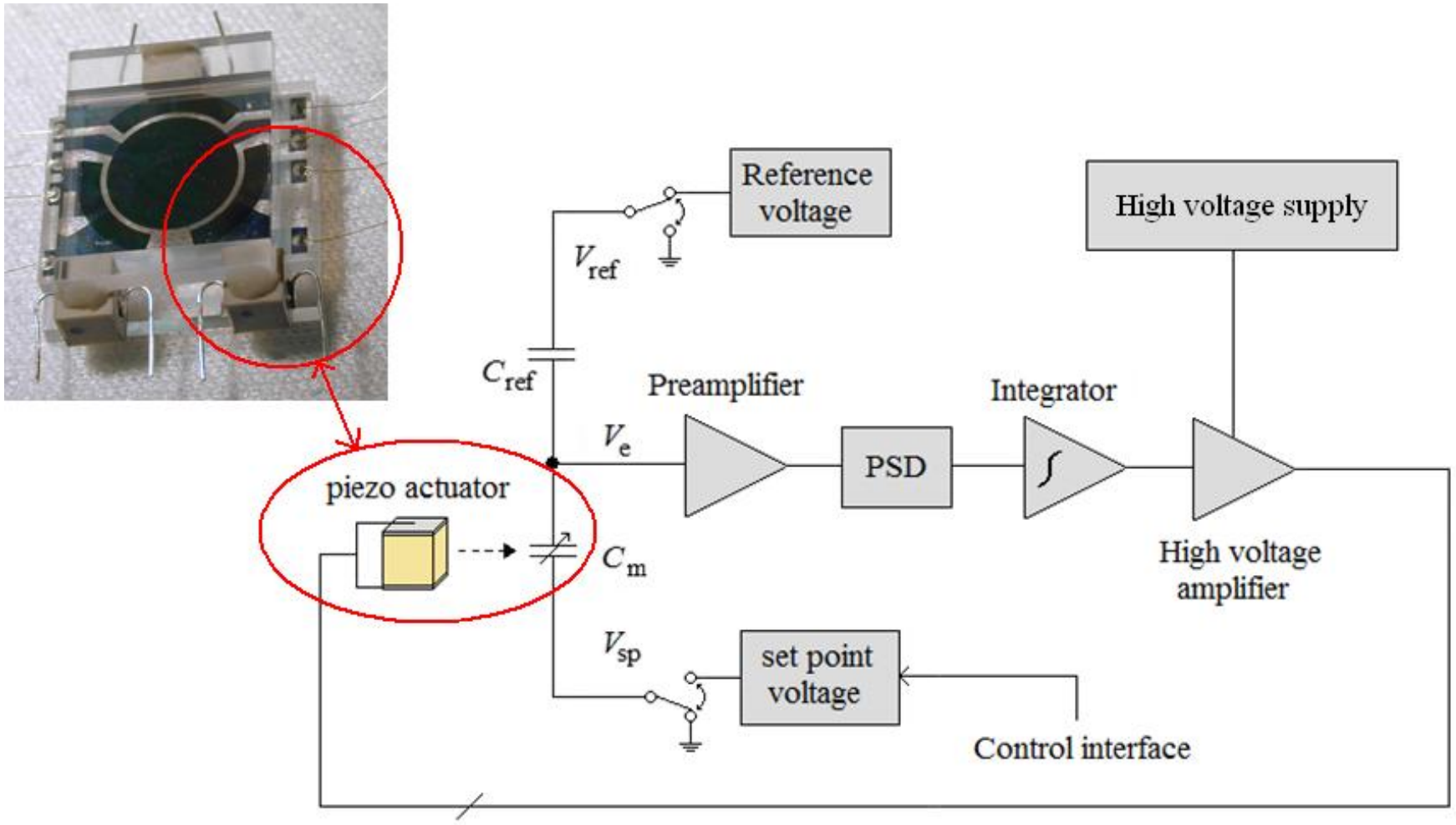

VTT's Surface Micro-Machined MEMS FPI Structure

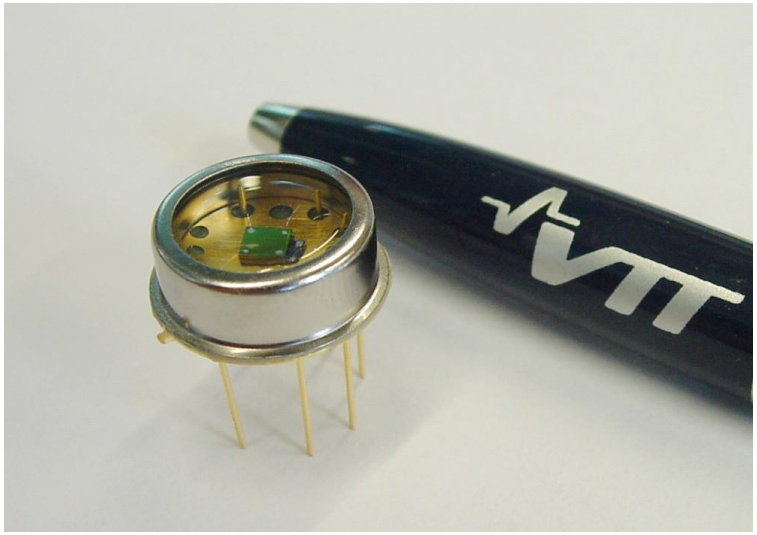

Upper mirror acts as a tensioned membrane → enables:

- Large optical apertures up to millimeters in diameter
- Superior mirror flatness
- Very high nominal frequencies, ~ 1 MHz (insensitive to vibrations)
- No gravitational effects
- Low operation voltages

World's first MEMS FPI Spectral Imager

- VTT has built world's first MEMS FPI based spectral imager device for demonstration to Photonics West 2011 fair
- The device consist of optics, a packaged MEMS Fabry-Perot Interferometer (aperture diameter 2 mm), and a color imager, together with electronics and mechanics.
- Device can be used for surface inspection (it has built-in white LEDs as light source) or in remote sensing mode, focused to infinity
- The wavelength range is 460-585 nm and resolution ca. 5 nm

FPI Spectral Imager trials with the UAV helicopter

- VTT has developed in previous VTT and Tekes funded projects proprietary hyperspectral imaging technology for light weight UAS planes (Patents: FI119345B , GB 2445956, Pat. Appl. FI20095356).
- A proof of concept prototype has been built and used in VITO (Flemish Institute for Technological Research) Draganfly X6 UAS helicopter.
- The results of the first trial flights has been published in SPIE conferences on September 2009[1] and April 2010[2].

VTT proof-of-concept prototype integration to the Draganfly X6 UÁS helicopter

VTT proof-of-concept prototype used for test targets onboard Draganfly X6 UÁS helicopter

[1]Saari, H., Aallos, V., Akujärvi, A., Antila, T., Holmlund C., Kantojärvi, U., Mäkynen, J. and Ollila J., "Novel Miniaturized Hyperspectral Sensor for UAV and Space Applications", Proc. SPIE 7474 (2009).

[2]Saari, H., Aallos, V., Holmlund, C., Mäkynen, J., Delauré, B., Nackaerts, K., and Michiels, B., "Novel Hyperspectral Imager for Lightweight UAVs", Proc. SPIE 7668 (2010) to be published.

VTT UAS FPI VIS-VNIR Spectral Camera for forest and agriculture applications

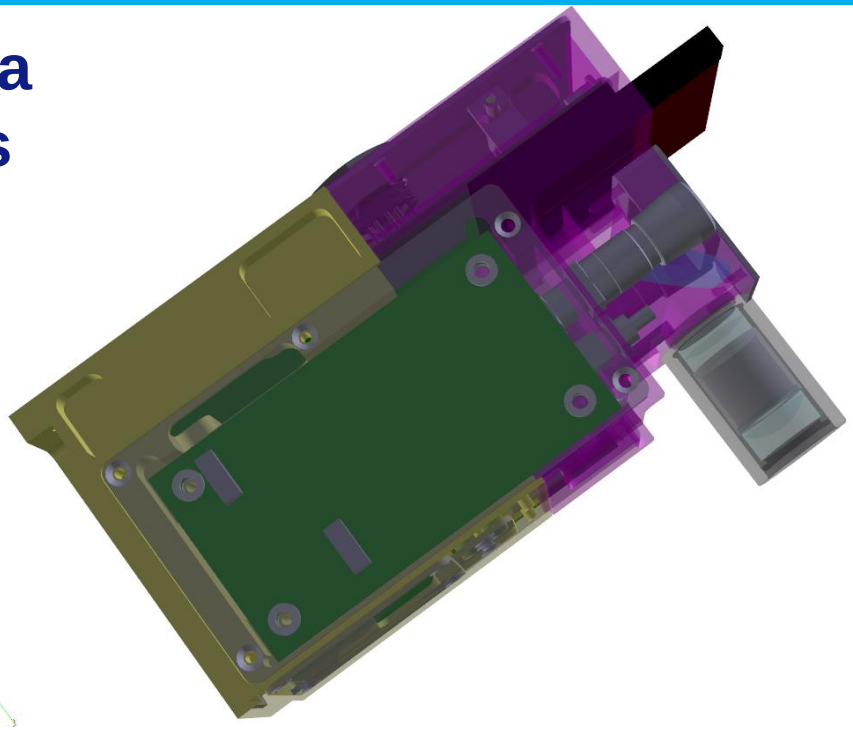

Major specifications of the spectral camera

Spectral range: 500 – 900 nm
Spectral Resolution: 7..10 nm @ FWHM
Focal length: 9.3 mm
Image size: 7.1 mm x 4.3 mm, 5 Mpix
Field of View: 32° (across the flight direction)
Ground pixel size: 3.5 cm @ 150 m height
Weight: 395 g
Size: 62 mm x 61 mm/76mm x 120 mm
Power consumption: 3 W

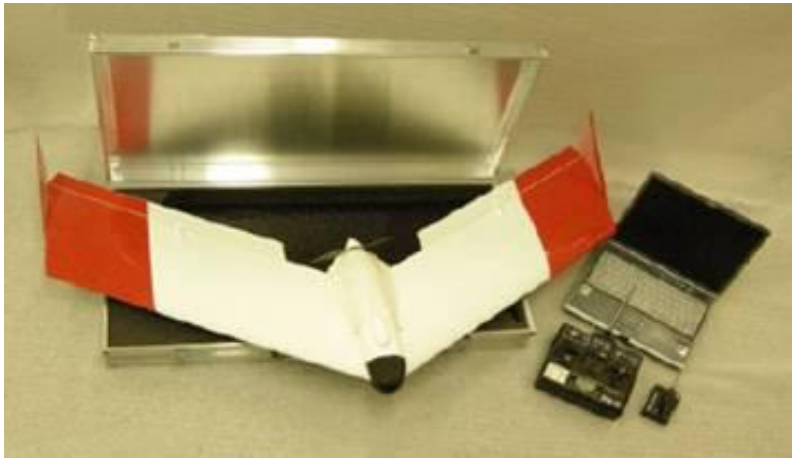

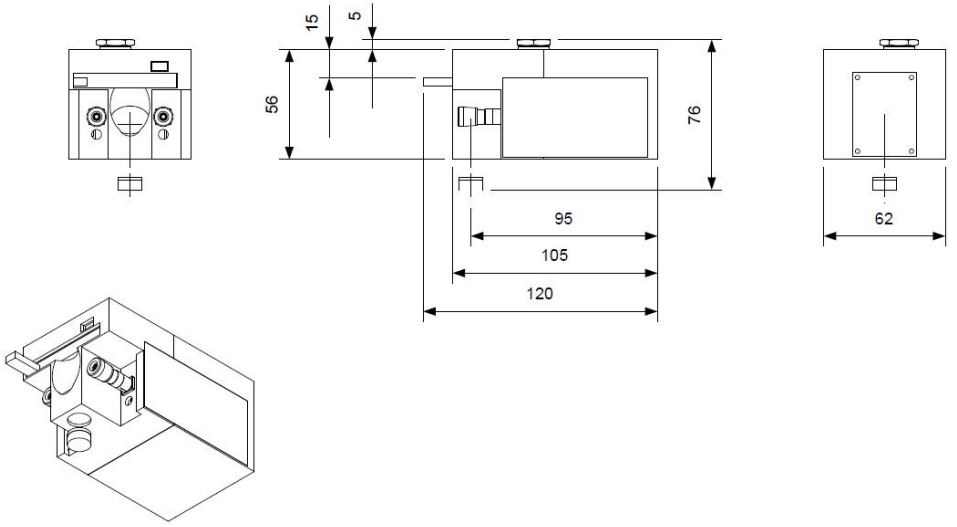

FPI based spectral camera F-number and throughput 1(4)

An ideal lens with focal length of f_{lens1} collimates the rays coming from an object with a height h_{im} and the angle of the collimated beam is θ_{max}. In the case of relay optics at magnification of 1 the $h_{im} = h_{cmos}$ which is the maximum radial height of the image sensor. It is now possible to calculate the focal length of the Lens 1

$$f_{Lens1} = \frac{h_{cmos}}{\tan(\theta_{max})} \qquad \text{Eq. 1}$$

The maximum effective aperture of the lens 1 can be approximated by the effective diameter of the FPI module D_{FPI}. The F-Number of the FPI spectral camera Fn_{sys1} is given by

$$Fn_{sys1} = \frac{h_{cmos}}{D_{FPI} \cdot \tan(\theta_{max})} \qquad \text{Eq. 2}$$

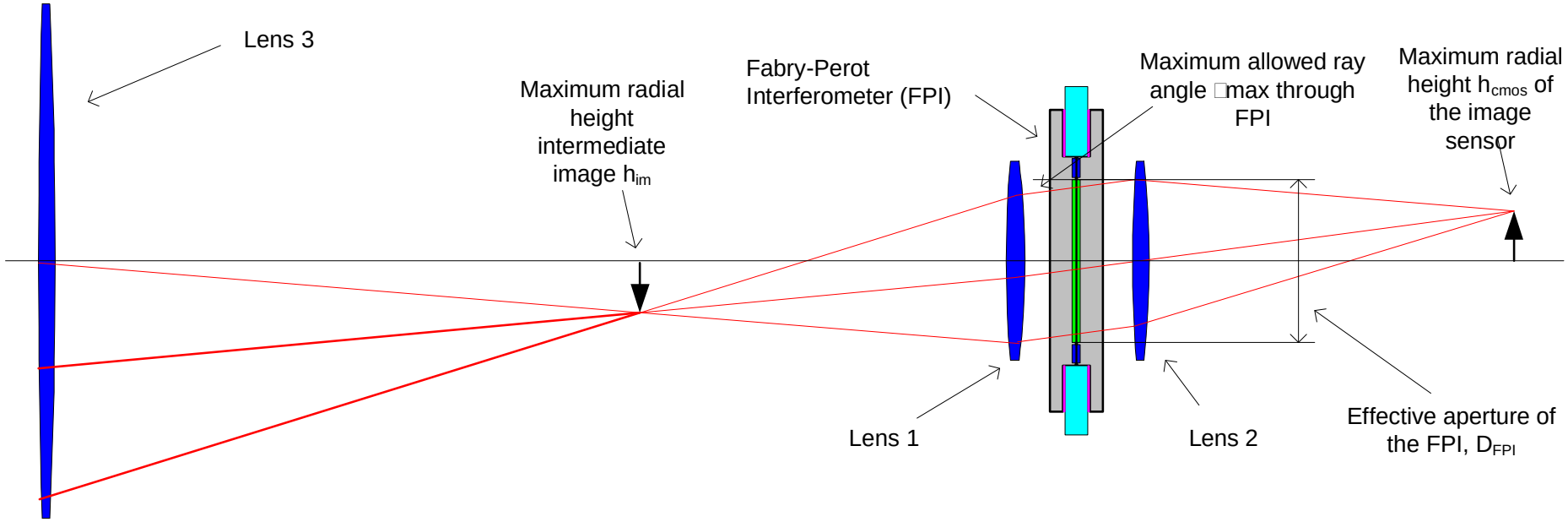

FPI based spectral camera F-number and throughput 2(4)

- It is possible to lower the F-number by using a larger FPI diameter and by increasing the max allowed FPI ray angle.
- The F-number as low as 1.0 can be achieved with 15 mm FPI diameter and 10 degree max FPI angle.
- This makes it possible to manufacture Hyperspectral imager with weight < 400 g for Vis-VNIR with F-number 1.0 and spectral resolution < 10 nm @ FWHM

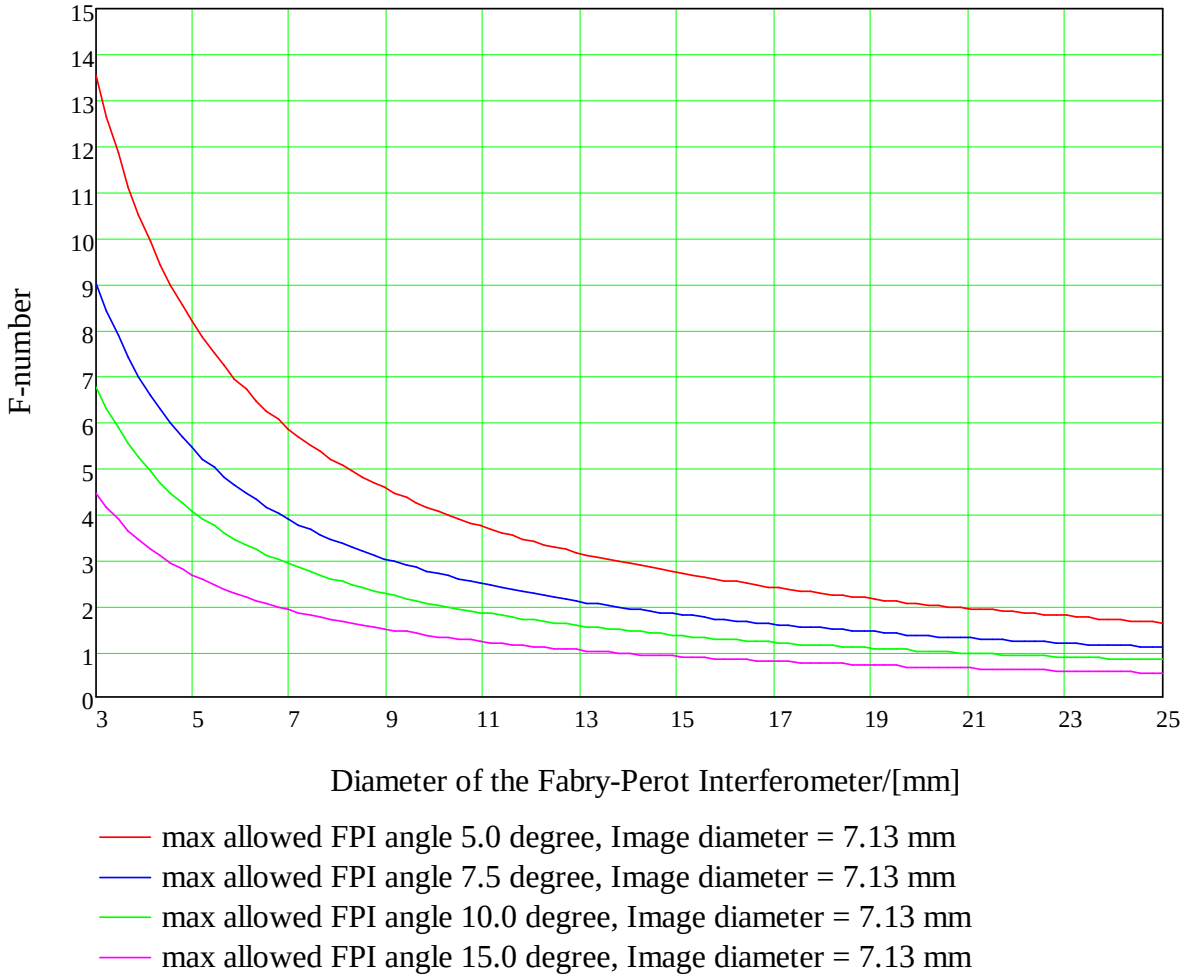

FPI based spectral camera F-number and throughput 3(4)

- The FPI ray angle affects the center wavelength of the FPI spectral peak. In the first approximation the peak wavelength is linearly dependent on the cosine of the ray angle.

$$\lambda_0 = \frac{m \cdot d \cdot \cos(\theta)}{2} \quad , \ \text{m=1,2....}$$

- The optics can be designed in such a way that the rays go through the FPI as a collimated beam for a specific pixel of the image.
- So for the measurement of continuous spectrum the large FPI ray angles can be used because the spectral resolution is not affected by the FPI ray angle

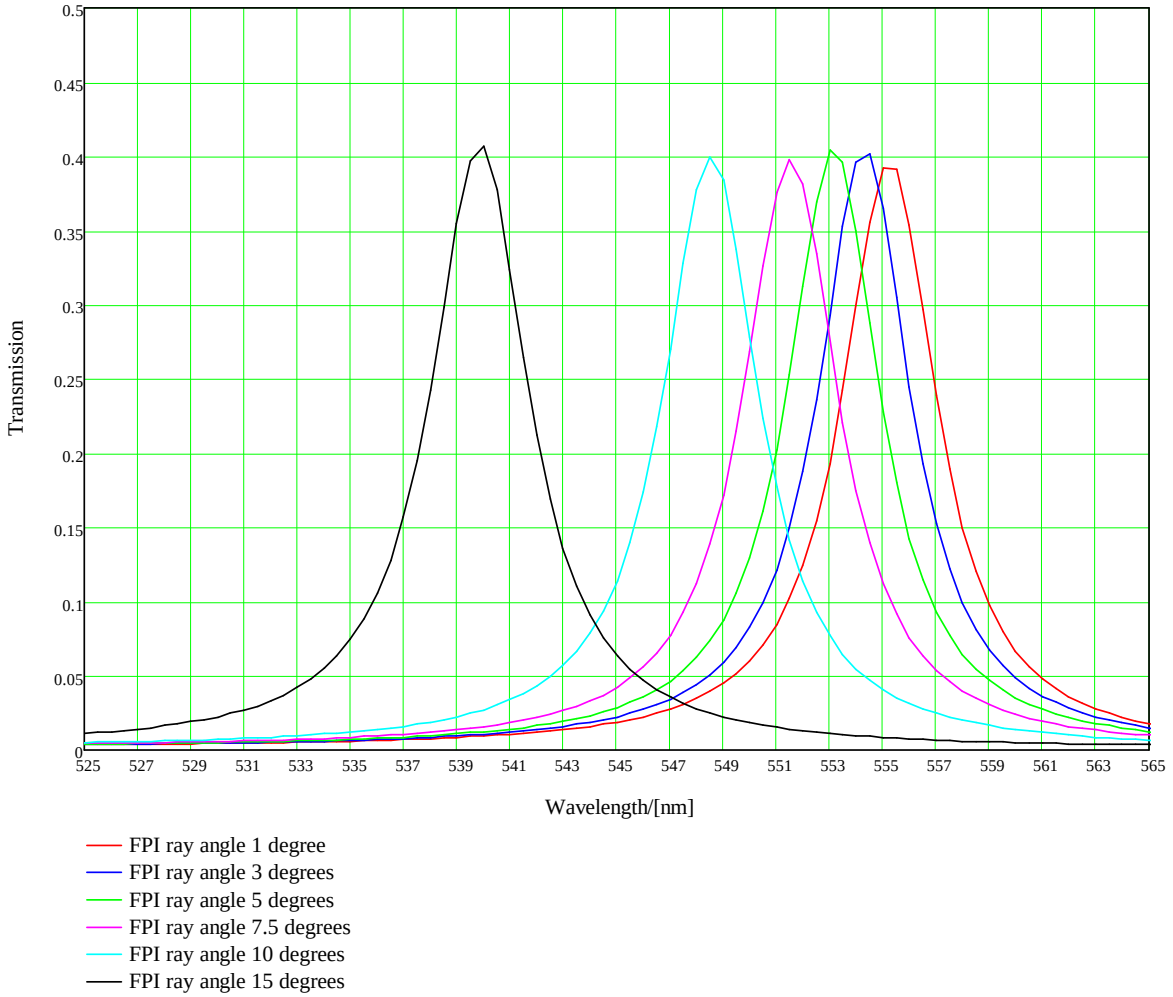

FPI based spectral camera F-number and throughput conclusions 4(4)

- The lowest F-numbers for existing push broom instruments are in the range 2.0….2.8 and the average transmission of the spectrograph is around 50% with peak transmission 70..80%.
- The FPI spectral imager average transmission with metal mirrors is around 25 % and 80 % with dielectric mirrors and lowest F-number in the range 1.0…1.8.

→ The throughput of FPI spectral imager can be higher than the throughput of push broom instruments if continuous spectrum is to be measured.

Signal of a RGB image sensor Blue (B), Green (G) and Red (R) pixels

Equations for the calculation of the signals of a RGB image sensor Blue (B), Green (G) and Red (R) pixels

$$S_B(d_{gap}) = \int_{\lambda_{min}}^{\lambda_{max}} \eta_B(\lambda) T_{FPI}(\lambda, d_{gap}) T_{sys}(\lambda) S(\lambda) d\lambda \quad \textbf{(5)}$$

$$S_G(d_{gap}) = \int_{\lambda_{min}}^{\lambda_{max}} \eta_G(\lambda) T_{FPI}(\lambda, d_{gap}) T_{sys}(\lambda) S(\lambda) d\lambda \quad \textbf{(6)}$$

$$S_R(d_{gap}) = \int_{\lambda_{min}}^{\lambda_{max}} \eta_R(\lambda) T_{FPI}(\lambda, d_{gap}) T_{sys}(\lambda) S(\lambda) d\lambda \quad (7)$$

$\eta_B(\lambda)$, $\eta_G(\lambda)$ ja $\eta_R(\lambda)$ are the quantum efficiences of the B-, G- ja R-pixels at the wavelength λ and the $S(\lambda)$ is the spectral photon flux entering the system. The combined spectral transmission of the optical system without the FPI is included in the term $T_{sys}(\lambda)$.

Retrieval of the spectral signals at the Fabry-Perot Interferometer pass bands at the selected three orders 1(3)

- For the retrieval of the spectral signal a calibration is required for the responses of the B-, G- and R-pixels around the selected three FPI pass bands.

$$S_{Bn}(d_{gap},n)=\int_{2\cdot d_{gap}\cdot(\frac{1}{n}-\frac{1}{2\cdot n\cdot(n+1)})}^{2\cdot d_{gap}\cdot(\frac{1}{n}+\frac{1}{2\cdot n\cdot(n-1)})}\eta_B(\lambda)T_{FPI}(\lambda,d_{gap})T_{sys}(\lambda)d\lambda$$

$$S_{Gn}(d_{gap},n)=\int_{2\cdot d_{gap}\cdot(\frac{1}{n}-\frac{1}{2\cdot n\cdot(n+1)})}^{2\cdot d_{gap}\cdot(\frac{1}{n}+\frac{1}{2\cdot n\cdot(n-1)})}\eta_G(\lambda)T_{FPI}(\lambda,d_{gap})T_{sys}(\lambda)d\lambda$$

$$S_{Rn}(d_{gap},n)=\int_{2\cdot d_{gap}\cdot(\frac{1}{n}-\frac{1}{2\cdot n\cdot(n+1)})}^{2\cdot d_{gap}\cdot(\frac{1}{n}+\frac{1}{2\cdot n\cdot(n-1)})}\eta_R(\lambda)T_{FPI}(\lambda,d_{gap})T_{sys}(\lambda)d\lambda$$

d_{gap} is the FPI air gap width, n is the FPI order, the $\eta_B(\lambda)$, $\eta_G(\lambda)$ ja $\eta_R(\lambda)$ are the quantum efficiences of the B-, G- ja R-pixels at the wavelength λ, $T_{FPI}(\lambda, d_{gap})$ is the spectral transmission of the FPI and $T_{sys}(\lambda)$ is the combined spectral transmission of the optical system without the FPI.

Retrieval of the spectral signals at the Fabry-Perot Interferometer pass bands at the selected three orders 2(3)

In a measurement the goal is to determine the spectral intensity S(λ) of the light
At a preset gap width we will measure signals S_{Bm}, S_{Gm} and S_{Rm}. at the B-, G- ja R pixels
The calibration coefficients S_{Bn}, S_{Bn+1}, S_{Bn+2}, S_{Gn}, S_{Gn+1}, S_{Gn+2}, S_{Rn}, S_{Rn+1} ja S_{Rn+2} can now be used for the calculation of the measured signals at the three narrow bands of three Fabry-Perot orders.
The measured signals of the light at the three FPI passbands are now

$$\begin{bmatrix} S_{Bn+2} & S_{Bn+1} & S_{Bn} \\ S_{Gn+2} & S_{Gn+1} & S_{Gn} \\ S_{Rn+2} & S_{Rn+1} & S_{Rn} \end{bmatrix} \cdot \begin{bmatrix} S_{n+2} \\ S_{n+1} \\ S_{n} \end{bmatrix} = \begin{bmatrix} S_{Bm} \\ S_{Gm} \\ S_{Rm} \end{bmatrix}$$

Where S_{n+2}, S_{n+1} and S_n are the unknown intensities at FPI orders n+2, n+1 and n.

The unknown can now be solved by

$$\cdot \begin{bmatrix} S_{n+2} \\ S_{n+1} \\ S_{n} \end{bmatrix} = \begin{bmatrix} S_{Bn+2} & S_{Bn+1} & S_{Bn} \\ S_{Gn+2} & S_{Gn+1} & S_{Gn} \\ S_{Rn+2} & S_{Rn+1} & S_{Rn} \end{bmatrix}^{-1} \cdot \begin{bmatrix} S_{Bm} \\ S_{Gm} \\ S_{Rm} \end{bmatrix}$$

Retrieval of the spectral signals at the Fabry-Perot Interferometer pass bands at the selected three orders 3(3)

The coefficients that must be applied to signals at B-, G- and R-pixels to get the signal at the selected air gap value are given by R matrix below

$$\begin{bmatrix} R_{Rn+2} & R_{Gn+2} & R_{Bn+2} \\ R_{Rn+1} & R_{Gn+1} & R_{Bn+1} \\ R_{Rn} & R_{Gn} & R_{Bn} \end{bmatrix} = \begin{bmatrix} S_{Rn+2} & S_{Rn+1} & S_{Rn} \\ S_{Gn+2} & S_{Gn+1} & S_{Gn} \\ S_{Bn+2} & S_{Bn+1} & S_{Bn} \end{bmatrix}^{-1}$$

The signal at the FPI order n+2 as a linear combination of the signals at B-, G- and R-pixels

The signal at the pass band of the FPI order n+2 is a linear combination of the signals at B-, G- and R-pixels.

$$S_{n+2} = R_{Rn+2} \cdot S_{Rm} + R_{Gn+2} \cdot S_{Gm} + R_{Bn+2} \cdot S_{Bm}$$

$$S_{n+2} = R_{Rn+2} \cdot \int_{\lambda_{\min}}^{\lambda_{\max}} \eta_R(\lambda) T_{FPI}(\lambda, d_{gap}) T_{sys}(\lambda) \Phi_{ph}(\lambda) d\lambda + R_{Gn+2} \cdot \int_{\lambda_{\min}}^{\lambda_{\max}} \eta_G(\lambda) T_{FPI}(\lambda, d_{gap}) T_{sys}(\lambda) \Phi_{ph}(\lambda) d\lambda + \quad (15)$$

$$R_{Bn+2} \cdot \int_{\lambda_{\min}}^{\lambda_{\max}} \eta_B(\lambda) T_{FPI}(\lambda, d_{gap}) T_{sys}(\lambda) \Phi_{ph}(\lambda) d\lambda$$

$$S_{n+2} = \int_{\lambda_{\min}}^{\lambda_{\max}} (R_{Rn+2} \cdot \eta_R(\lambda) + R_{Gn+2} \cdot \eta_G(\lambda) + R_{Bn+2} \cdot \eta_B(\lambda)) \cdot T_{FPI}(\lambda, d_{gap}) T_{sys}(\lambda) \Phi_{ph}(\lambda) d\lambda$$

Calibration of the FPI Hyperspectral Imager 1(5)

The calibration should provide as an output the spectral response curves

$$\eta_R(\lambda)\cdot T_{FPI}(\lambda, d_{gap})\cdot T_{sys}(\lambda),\ \eta_G(\lambda)\cdot T_{FPI}(\lambda, d_{gap})\cdot T_{sys}(\lambda),\ \eta_B(\lambda)\cdot T_{FPI}(\lambda, d_{gap})\cdot T_{sys}(\lambda)$$

These curves are used in the calculation of the calibration coefficients S_{Bn}, S_{Bn+1}, S_{Bn+2}, S_{Gn}, S_{Gn+1}, S_{Gn+2}, S_{Rn}, S_{Rn+1} and S_{Rn+2}.

The coefficients R_{Bn+1}, R_{Bn+2}, R_{Gn}, R_{Gn+1}, R_{Gn+2}, R_{Rn}, R_{Rn+1} and R_{Rn+2} are derived as an inverse matrix of S-coefficients.

The R-coefficients can be used in the calculation of photon flux at the three spectral bands of FPI orders n+2, n+1 and n.

Calibration of the FPI Hyperspectral Imager 2(5)

- The calibration is started with the measurement of the spectral photon flux entering the input of the FPI spectral imager.

- The signals of the absolute radiometer and the reference detector are typically recorded for wavelength ranges 400 – 1000 nm at 1 nm intervals and at a resolution of 1 @ FWHM.

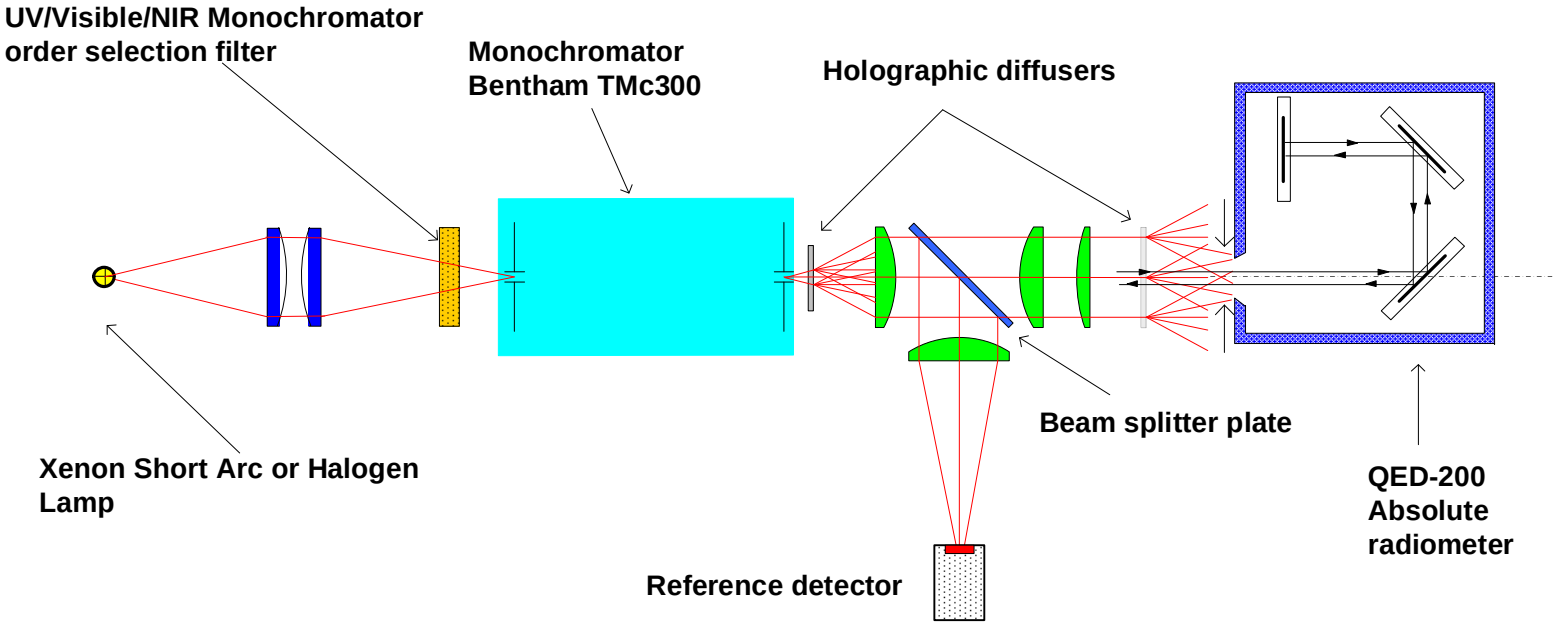

Absolute photon flux calibration detector
Three photodiode light trap photodetector QED-200-14526
(Calibrated absolute photometer for quantum efficiency measurements)

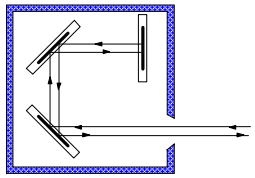

Calibration of the FPI Hyperspectral Imager 3(5)

The calibration measurement for the FPI hyperspectral image sensor is performed by recording for each selected air gap value the images of the RGB image sensor for the same spectral range and at the same spectral step and slit width as in the calibration of the spectral photon flux.

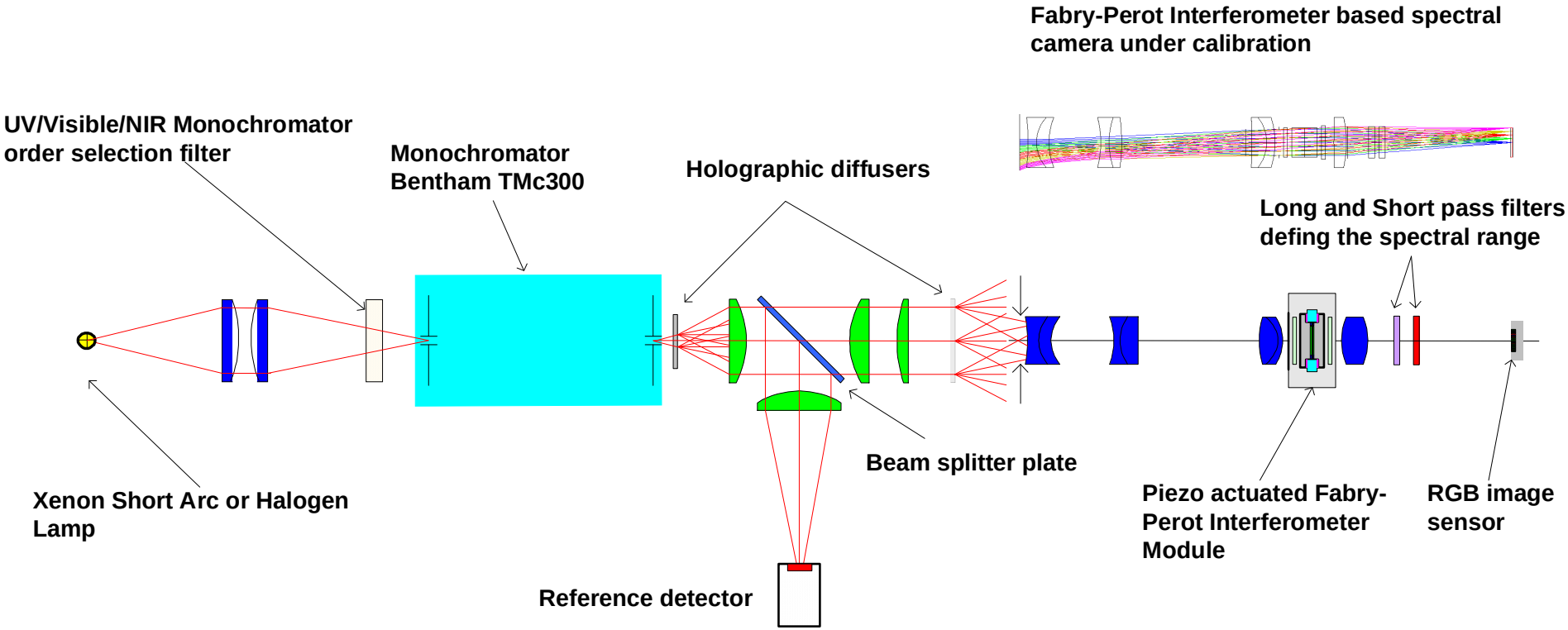

Calibration of the FPI Hyperspectral Imager 4(5)

Because the spectral photon flux $\Phi_{ph}(\lambda)$ is known it is possible determine for hyperspectral image sensor total spectral response i.e. product $K_{ADU} \cdot T_{FPI}(\lambda, d_{gap}) \cdot T_{sys}(\lambda) \cdot \eta(\lambda) = S_{sys}(\lambda)$ for R-, G-, and B-pixels

$$S_{sys}(\lambda) = \frac{K_{ADU} \cdot \eta_R(\lambda) T_{FPI}(\lambda, d_{gap}) T_{sys}(\lambda) \Phi_{ph}(\lambda)}{\Phi_{ph}(\lambda)} = K_{ADU} \cdot \eta_R(\lambda) T_{FPI}(\lambda, d_{gap}) T_{sys}(\lambda)$$

The system gain K_{ADU} is the total gain of the image sensor in units ADU/electrons which can be determined using the mean-variance method. The sensitivity in equation above is given in absolute units ADU/photons.

Typical result of a FPI Hyperspectral Imager Calibration

- Measured total spectral sensitivity of R-, G-, and B-pixels at air gap value 1400 nm
- Spectral resolution is 7 – 9 nm @ FWHM

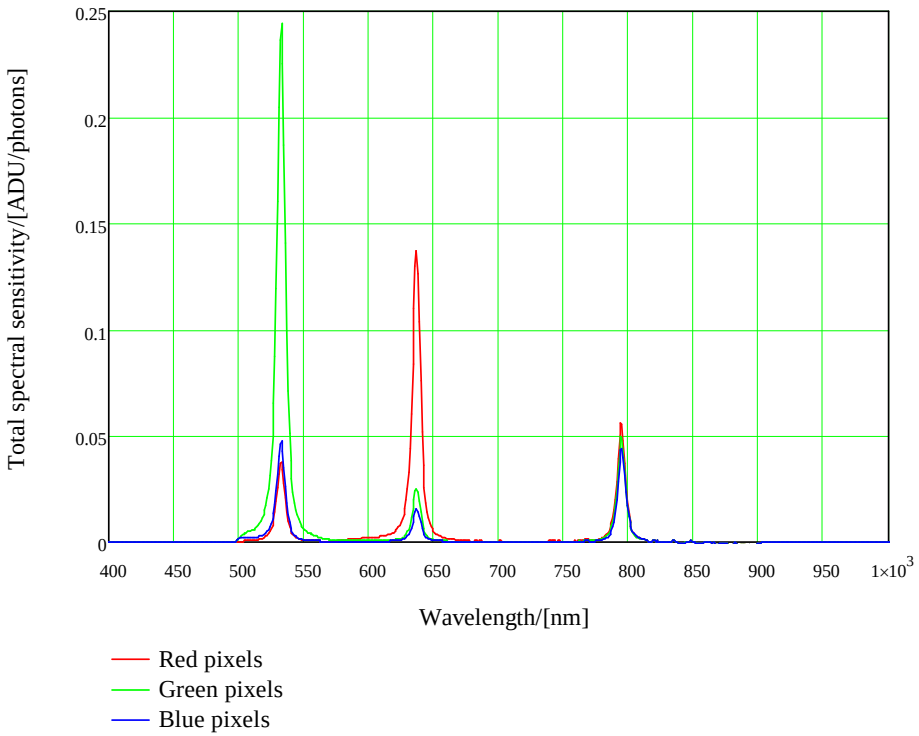

- Measured total spectral sensitivity at spectral peak of FPI order n+2 at air gap value 1400 nm.
- The total spectral sensitivity is derived as a weighted sum of the R-, G-, and B-pixel sensitivities plotted on the left.
- The weights were taken from R-matrix for FPI air gap 1400nm. R-pixel weight =-0.154 , G-pixel weight = 2.098 and B-pixel weight = -2.184

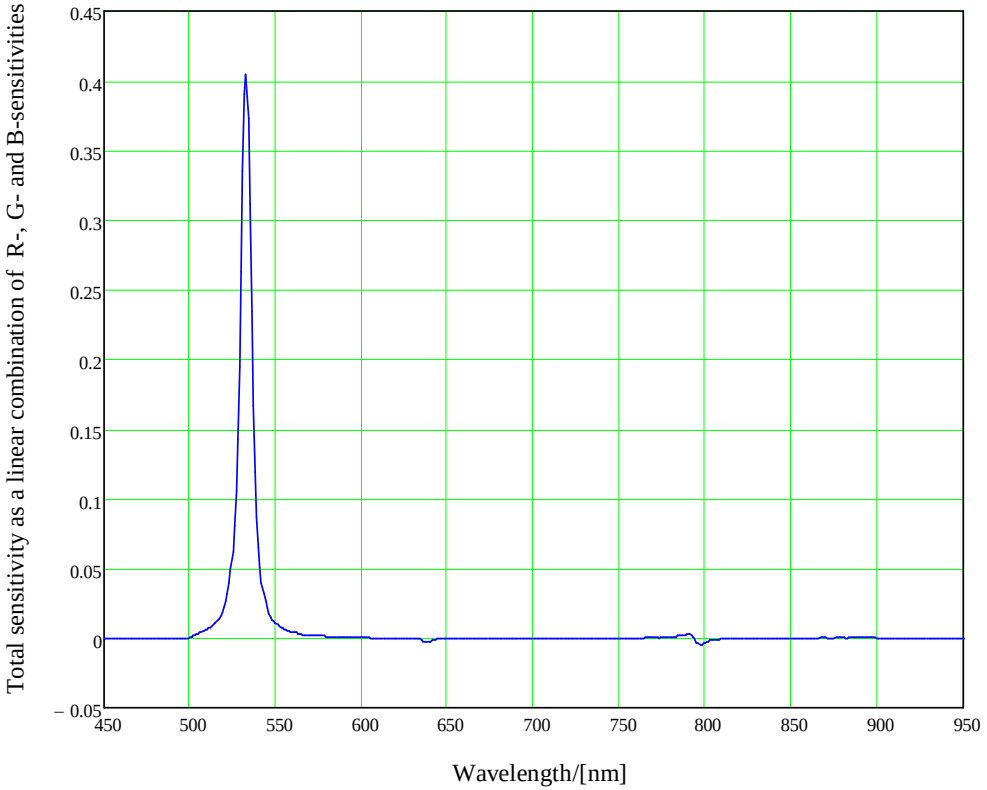

SNR estimation for the FPI Hyperspectral Imager

The total spectral sensitivity function for one specific spectral band representing one FPI order at a fixed FPI air gap can be expressed with Equation

$$I(\lambda) = (R_{Rn+2} \cdot \eta_R(\lambda) + R_{Gn+2} \cdot \eta_G(\lambda) + R_{Bn+2} \cdot \eta_B(\lambda)) \cdot T_{FPI}(\lambda, d_{gap}) T_{sys}(\lambda)$$

If we assume a constant signal over the whole spectral range we get for the signal at the spectral peak of FPI order n+2 (λ_{n+2}) S_{n+2}

$$S_{n+2} = \int_{\lambda_{n+2}-\Delta\lambda}^{\lambda_{n+2}+\Delta\lambda} (R_{Rn+2} \cdot \eta_R(\lambda) + R_{Gn+2} \cdot \eta_G(\lambda) + R_{Bn+2} \cdot \eta_B(\lambda)) \cdot T_{FPI}(\lambda, d_{gap}) T_{sys}(\lambda) \Phi_{ph}(\lambda) d\lambda$$

The square of the noise $(N_{n+2})^2$ can be estimated with the following

$$N_{n+2}^2 = \int_{\lambda_{min}}^{\lambda_{n+2}-\Delta\lambda} ((R_{Rn+2} \cdot \eta_R(\lambda) + R_{Gn+2} \cdot \eta_G(\lambda) + R_{Bn+2} \cdot \eta_B(\lambda)) \cdot T_{FPI}(\lambda, d_{gap}) T_{sys}(\lambda) \Phi_{ph}(\lambda))^2 d\lambda +$$

$$\int_{\lambda_{n+2}+\Delta\lambda}^{\lambda_{max}} ((R_{Rn+2} \cdot \eta_R(\lambda) + R_{Gn+2} \cdot \eta_G(\lambda) + R_{Bn+2} \cdot \eta_B(\lambda)) \cdot T_{FPI}(\lambda, d_{gap}) T_{sys}(\lambda) \Phi_{ph}(\lambda))^2 d\lambda$$

Where $\Delta\lambda$ is width of the spectral peak defined in such a way that the signal is contained in the range $\lambda_{n+2} - \Delta\lambda - \lambda_{n+2} + \Delta\lambda$. The relevant spectral range $\lambda_{min} \leq \lambda \leq \lambda_{max}$ is determined with long and short pass filters. The Signal-to-Noise-Ratio (SNR_{n+2}) can now be expressed as

$$SNR_{n+2} = \frac{S_{n+2}}{N_{n+2}}$$

Example of the SNR estimation for the FPI Hyperspectral Imager

- Simulated peak wavelengths and SNR at the highest FPI order used as a function of the FPI air gap. The spectral band is limited to 500 – 900 nm with filters.
- At low FPI air gap values (100 – 550 nm) there is only one FPI order wavelength and the SNR value is large.
- The SNR value drops near the air gap values at which a spectral peak is appearing at the edges of the long or short pass filter pass band.

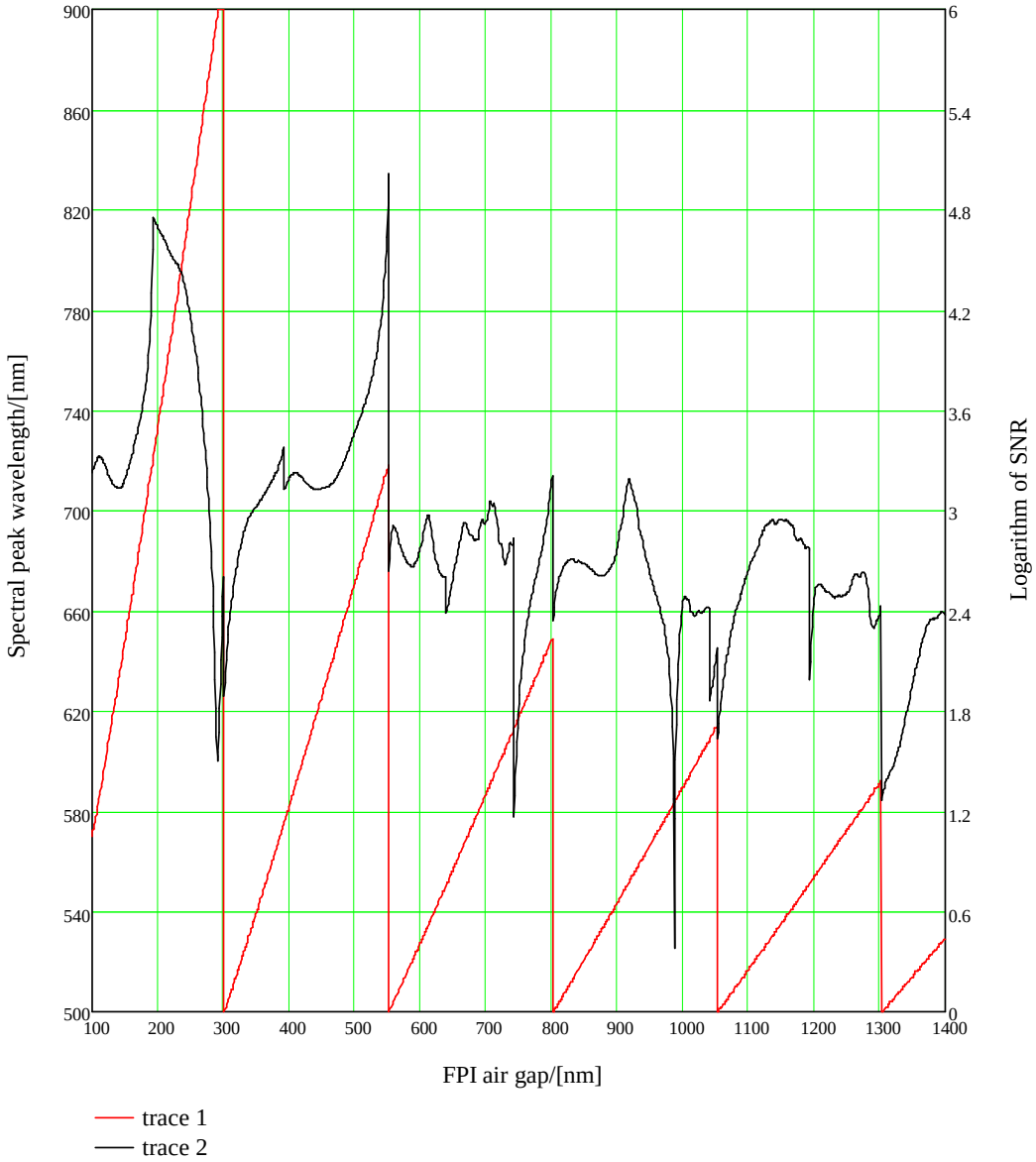

Devices built based on the piezo-FPIs

- **Chemical Imager (1-2.5 µm)**
  - Malinen, J. et.al., “Comparative performance studies between tunable filter and pushbroom chemical imaging systems”, Proc. SPIE 7680 (2010).
- **Handheld hyperspectral imager (400-700 nm)**
  - Saari, H. et.al., “Hand-Held Hyperspectral Imager”, Proc. SPIE 7680 (2010).
- **Light-weight hyperspectral imager for UAVs (500-900 nm)**
  - Saari, H. et.al., “Novel Hyperspectral Imager for Lightweight UAVs”, Proc. SPIE 7668 (2010)
- **Handheld hyperspectral imager for remote sensing, food quality and medical applications**
  - Saari, H. et.al. Handheld spectral imager for remote sensing, food quality and medical applications. Proceedings of Finnish Remote Sensing Days 3.-4.11.2010.

Applications

- The light weight and framing imaging mode enable totally new applications for the hyperspectral imaging because cost effective UAVs can be used to acquire data.
- The remote sensing applications that can benefit from the new UAV instrument include precision agriculture, forestry, natural water monitoring applications.
- In space the need of compact hyperspectral imager has been also been identified and the new technology to manufacture RGB-type pixelized multispectral image sensors for wide spectral range including IR enables the development of a highly compact hyperspectral imager for SWIR (1.0 – 3.0 µm) range using MCT detector & multispectral filter in combination of Fabry-Perot interferometer.
- The hyperspectral imaging has been used in medical imaging, accurate color measurements, pharmaceutical manufacturing, diagnostic test analysis equipment, art restoration, archaeology etc.
- The presented new concept has potential to offer hyperspectral imaging system at a much lower cost level opening many applications in which it has been previously blocked by the cost of hardware.

Conclusions and future plans

- The Fabry-Perot Interferometer technology has been developed at VTT to level that it can be used in hyperspectral imagers
- In many applications it is beneficial to produce megapixel 2D spatial images with a single exposure at a few selected wavelength bands instead of 1D spatial and all spectral band images like in push broom instruments.
- In this spectrometer the multiple orders of the Fabry-Perot Interferometer are used at the same time matched to the sensitivities of the multispectral image sensor wavelength channels.
- The F-number of the spectral camera can be as low as 1.0 for cases were full spectral data cube is to be measured.
- The size (< 65 mm x 65 mm x 120 mm), weight (< 400 g) and power consumption (< 3 W) of the FPI hyperspectral spectrometer is compatible with the light weight UAV platforms.
- The Finnish Aalto-1 Nanosatellite Payload will be based on the MEMS FPI hyperspectral imager.

Contacts

Heikki Saari
VTT Photonic Devices and Measurement Solutions
PL1000, Espoo, Finland
Phone: +358 40 5891254
Email: heikki.saari@vtt.fi

Additional slides on the-state-of-the-art of the hyper and multispectral imaging technology and on planned UAV applications of Fabry-Perot Interferometer spectral imager

State-of-the-art in multi&hyperspectral imaging

- New multispectral technologies are being developed by companies like Ocean Optics, Silios, etc.
- The Rotating Filter Wheel (RFW) Multispectral Camera technology has developed with small steps during recent years.
- The new opportunities is offered by the Dichroic Filter Array (DFA) Multispectral Camera technology presented by Ocean Optics at the SPIE conference "Imaging, Manipulation, and Analysis of Biomolecules, Cells, and Tissues VIII" SPIE Vol.7568.
- VTT has developed MEMS Fabry-Perot Interferometers for the visible wavelength range. This technology is planned to be used in the Finnish Aalto-1 nanosatellite for hyperspectral remote sensing.
- The combination of a MEMS FPI and a dichroic filter array would enable to build a hyperspectral imager whose spectral bands could be tuned to various applications.

Rotating Filter Wheel (RFW) Multispectral Camera

- Multispectral imaging has traditionally been performed with rotating filter wheel.
- If the wavelength bands required for the application are known the RFW multispectral imager is a straight forward solution.
- The disadvantages of the RFW concept are
  - Tuning of the spectral bands is not possible
  - The spectral bands are registered at different times
  - The miniaturization is challanging because of the filter wheel mechanism.

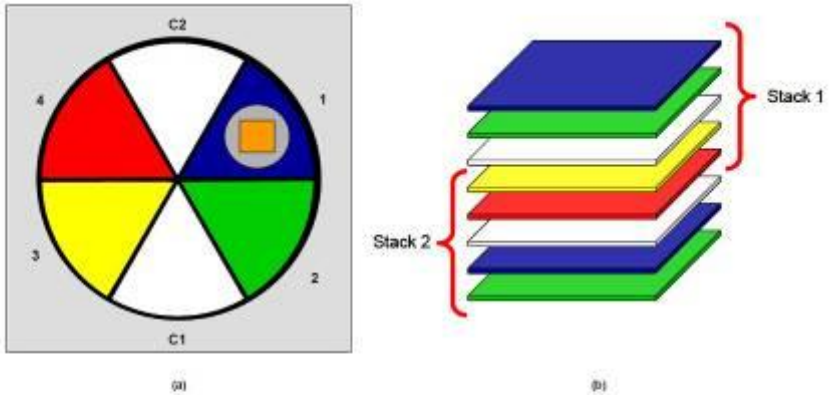

Figure 3. Rotation of the filter wheel and stacking of the data into the image stack for image stabilization and processing

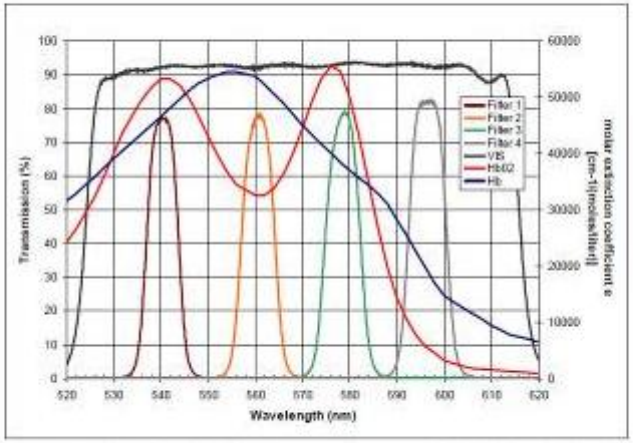

Figure 2. RFW pass bands overlaid with the key blood oxygenation curves of the initial application. Note the >75% pass band for the filters (Filter1-Filter4), as well as the visible blocking filter (VIS). Also shown are molar extinction curves in cm^{-1}/(moles/liter)

Ref. Eichenholz, J.M., et.al., “Real time Megapixel Multispectral Bioimaging”, Proc. SPIE 7568 (2010).

Dichroic Filter Array (DFA) Multispectral Camera

- The physical size of the DFA is 35 mm x 23 mm and there are 3500x2500 individual filters on the DFA. The pixel pitch is 10 µm x 10 µm.
- The image of a target is formed on the DFA surface and the Microscope objective forms an image of the DFA on the Camera sensor.
- The advantages of DFA camera are
  - The spectral bands are registered simultaneously
  - No moving parts
- The disadvantages of the DFA concept are
  - Tuning of the spectral bands is not possible
  - The miniaturization is challenging because of relay optics required for imaging the DFA to the image sensor.

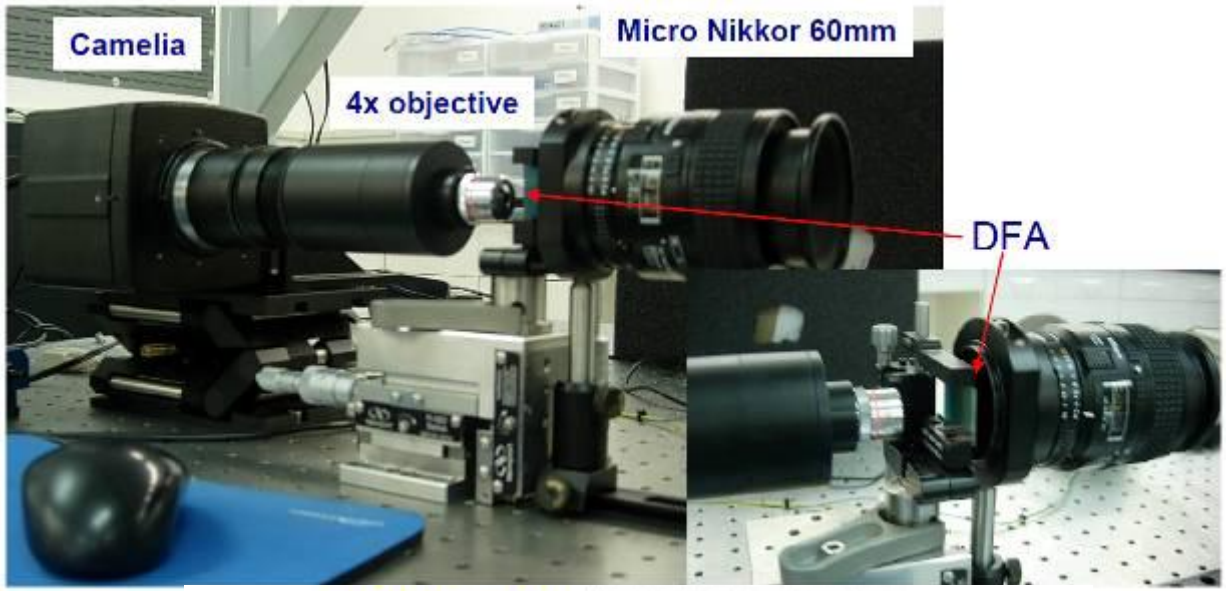

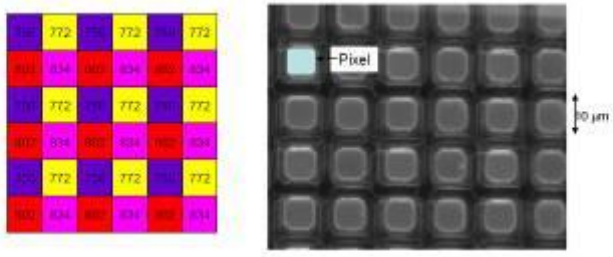

Figure 5. (a) Bayer like pattern and (b) microscope image of the dichroic filter array.

The physical size of the DFA is 35 mm x 23 mm. There are 8.75 Million (3500x2500) individual filters on each DFA. Each individual pixel is 10 µm x 10 µm on a 10 µm center to center spacing with a 1 micron border around the edge of each pixel resulting in an active area of 8 µm x 8 µm. A microscope transmission image of a small section of the DFA is shown above in Figure 5b.

Ref. Eichenholz, J.M., et.al., “Real time Megapixel Multispectral Bioimaging”, Proc. SPIE 7568 (2010).

Hyperspectral imager concept based on combining a Dichroic Filter Array with Fabry-Perot Interferometer

Patterned dielectric multispectral filter array integrated with a IR detector

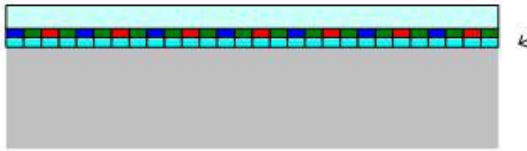

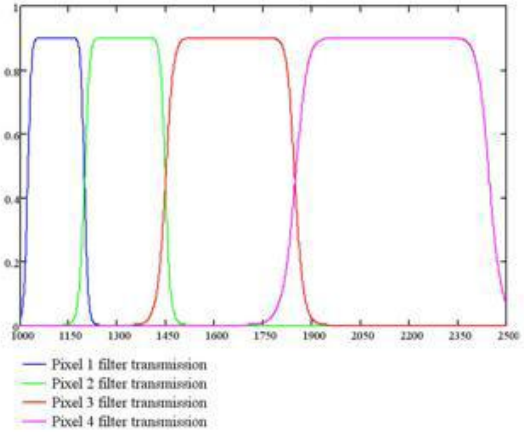

Combined spectral transmission of Patterned dielectric multispectral filter array and Fabry-Perot Interferometer used at 4 orders

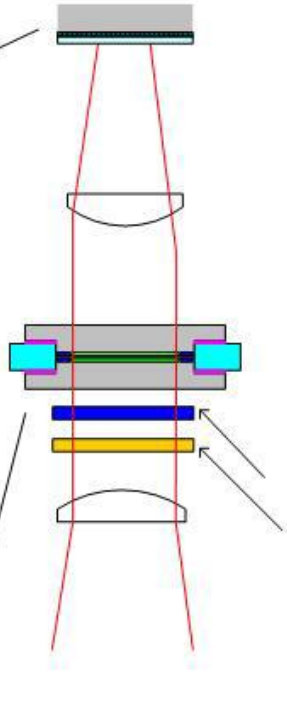

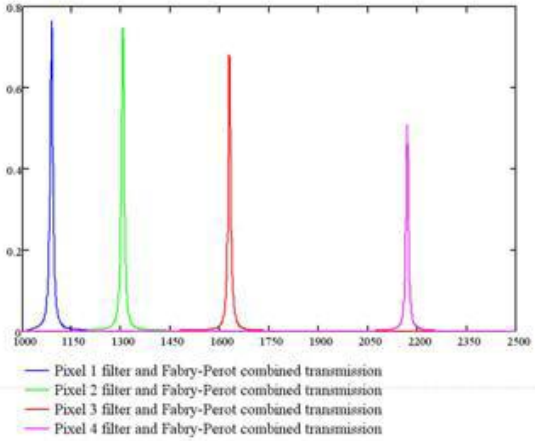

High Pass Filter

Low Pass Filter

One can separate the multiple order peaks by using special filters!

Piezoactuated Fabry-Perot Interferometer module

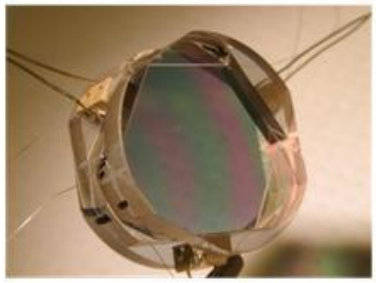

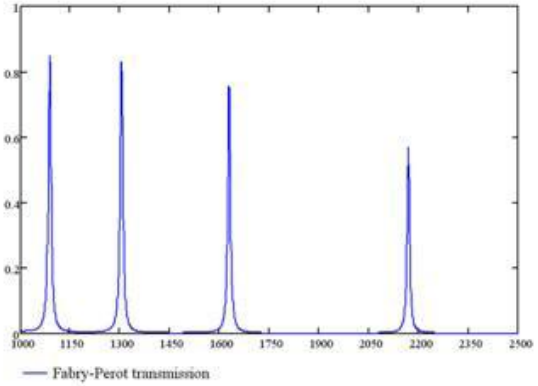

Application of spectral imaging in crop farming - Information flow is marked with numbers

FARMER

Enchanhed farming and production planning
- saves in fertilizer, watering & other costs
- Product quality > price
- Environmental issues

INDUSTRY

Forecasting and traceability data (contracts)
Amount and quality of crop yield

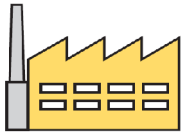

WEB data bases for farmers data

1. 6.

Aerial images
Interpreted images

6.

INFORMATION SERVICES/ FARMING PROGRAMS

Spectral libraries for interpretation
Support for interpretation and farming planning
manual&automatic

DATA FOR A FARM

2. 4.

3.

Research
Support for product development

Planning maps
Actual maps

5.

Weather and other ambient env. data

6.

ADMINISTRATION

Knowledge on the validity of the EU support conditions

Aerial images

FARMING TASKS

FERTILIZING

SPRAYING

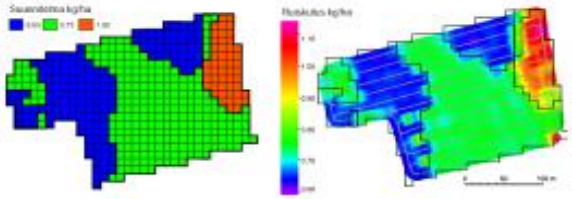

Application of spectral imaging in forestry applications- Information flow is marked with numbers

Forest officer/Forest usage planner

Cutting planning
-stand based tree volume and
-tree species data to PC
- More accurate cutting plan
saving cost in cutting work

Aerial images

Stand based data

Weather and other ambient env. data

WEB-DATABASES
Forest Remote Sensing data

Aerial images
Interpreted images

1.

2.

3.

Cutting plan

Borders of the area to be cut
- Image data of the forest area
- tree volume and species data

4.

Cutting of forest

5.

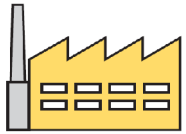

INDUSTRY

Forecasting and traceability data (contracts) amount, species and quality of cut trees

6.

INFORMATION SERVICES

Interpretation + forest usage planning

RESEARCH

Spectral data bases

6.

ADMINISTRATION

Knowledge on the validity of the EU support conditions

Aalto-1 Nanosatellite Payload Overview

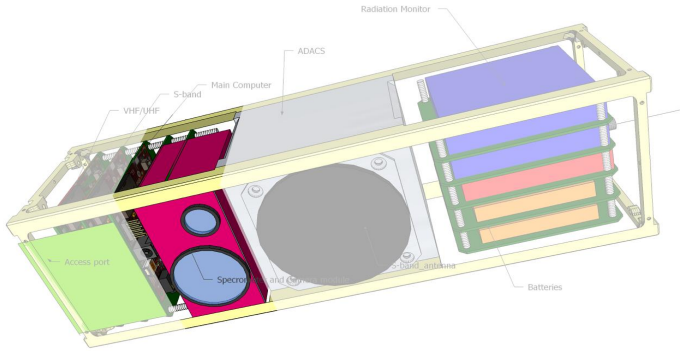

- A miniature Hyperspectral Imager based on a tunable Fabry-Pérot interferometer
- Joint project between Aalto-university and VTT Technical Research Centre of Finland
- The spectrometer module is built and developed by VTT Technical Research Centre of Finland
- The spectral imager is accompanied by a high resolution digital camera
- The smallest hyperspectral imager to be used in a satellite

Spectral imaging for the monitoring of Wine leave health status

- Wine grapes are robust plants that can live more than 100 years but, depending on the atmospheric conditions, they may be attacked by several different plagues or diseases along their lives, or even by hailstorms. And all these problems affect in different ways to the quality of the grapes growing on those wines and, consequently in the long run, to the wine.
- Spectral imaging experiments were planned to detect Mildew on Wine leaves
- Downy Mildew is a disease that can be extremely serious in grapes and will cause severe crop loss. The fungus Plasmopara viticola causes downy mildew.

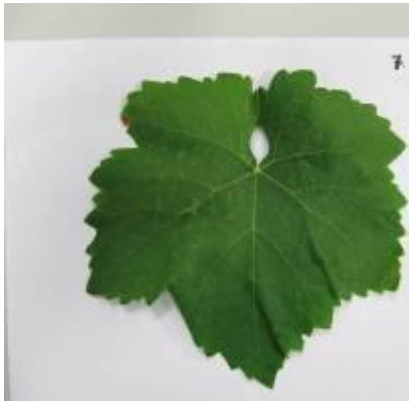

Case 2: Spectral imaging in clinical processes especially brain surgery 1(2)

Cedip IR camera

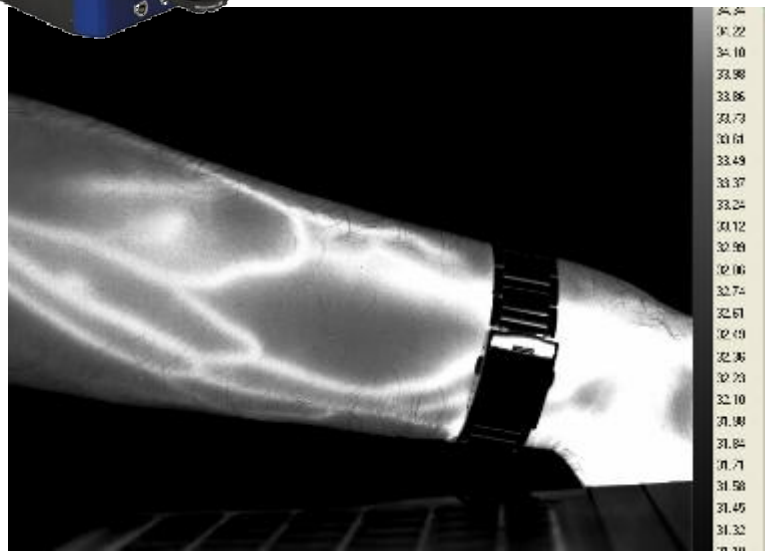

Brain tumour surgery under mouth-controlled operating microscope

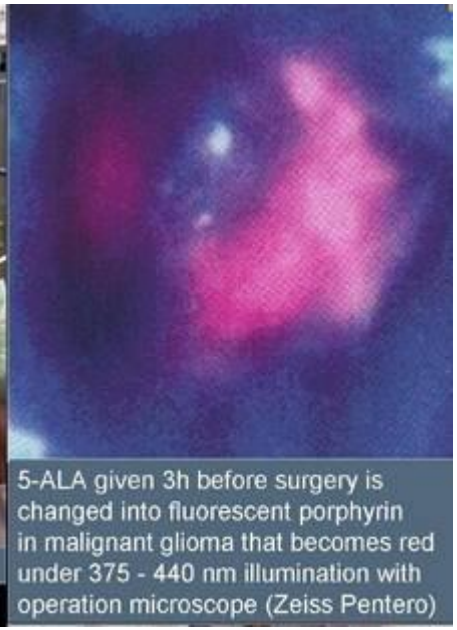

5-ALA given 3h before surgery is changed into fluorescent porphyrin in malignant glioma that becomes red under 375 - 440 nm illumination with operation microscope (Zeiss Pentero)

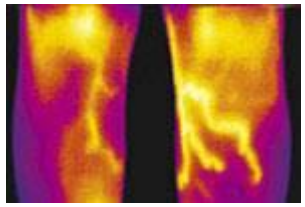

http://www.flir.com/thermography/eurasia/en/

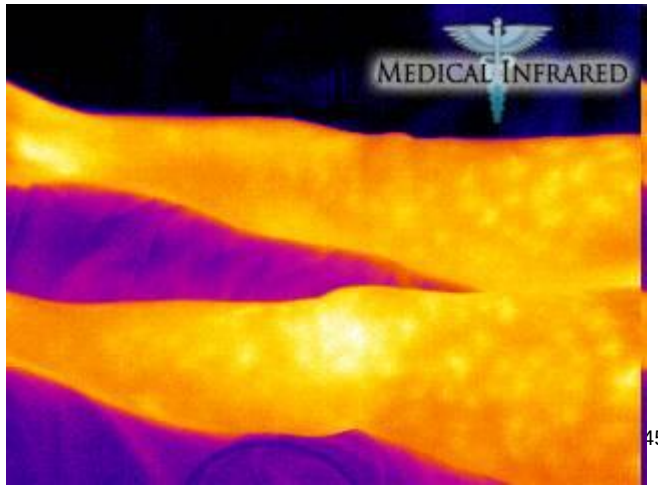

Infrared thermal Image of deep vein Thrombphlebitu on the left leg

http://www.infraredcamerasinc.com

Case 2: Spectral imaging in clinical processes especially brain surgery 2(2)

- In the MEDI-IMAGING project Fabry-Perot Interferometer Spectral camera will be integrated to the Zeiss Pentero brain surgery microscope.
- The spectral range used in the study is 400 – 1000 nm.

The spectral camera is planned to be integrated to the Zeiss pentero brain surgery microscope at the Kuopio University Hospital